16th World Conference on Earthquake Engineering, 16WCEE 2017
Santiago Chile, January 9th to 13th 2017
Paper N° 2120
Registration Code: S-B1461860701

REDUCTION OF LIQUEFACTION-INDUCED KINEMATIC PILE LOADING BY MEANS OF IN-GROUND RINGWALL

J. Go[1], R. Gibson[2], J. Lopez[3], Z. Lubkowski[4]

[1] Associate, Arup, Infrastructure, London, James.Go@arup.com
[2] Associate, Arup, Advanced Technology & Research, London, Rupert.Gibson@arup.com
[3] Engineer, Arup, Infrastructure, London, Jorge.Lopez@arup.com
[4] Associate Director, Arup, Infrastructure, London, Ziggy.Lubkowski@arup.com

Abstract

This paper presents an approach to reducing liquefaction-induced kinematic loading on piles by means of an in-ground ringwall made of overlapping jet grout columns. A vulnerability assessment using Dynamic Soil-Structure Interaction (DSSI) analysis of the pile foundation of an existing liquefied petroleum gas (LPG) spherical storage tank has identified that the piles capacity will be exceeded during a design earthquake. Liquefaction assessment indicated that several soil layers may liquefy and create non-liquefied 'crusts' that impose additional lateral deformation along the length of the pile. The precast pre-stressed concrete piles had relatively low lateral capacity and were prone to bending failure during earthquake shaking.

A retrofit study was performed to assess the effectiveness of an in-ground wall concept in minimizing the kinematic loads on the piles. The concept was to construct overlapping jet grout columns that form a ringwall that would deflect the kinematic loading of the non-liquefied 'crusts', shielding the brittle piles during earthquake shaking. To help select efficient ringwall configurations, several pushover analyses were performed varying the ringwall thickness and depth. Finally, the optimized ringwall configurations were incorporated into the full DSSI model and subjected to two orthogonal horizontal acceleration time histories. Results indicated that the in-ground ringwall greatly reduced the kinematic loading on the piles, and hence piles that once failed now perform within capacity. The DSSI analyses provided 'proof of concept' that shows in-ground walls reduce kinematic loading and can be used to retrofit the existing foundations.

Keywords: dynamic soil-structure interaction; kinematic loading; pile foundations; liquefaction mitigation; petrochemical facilities.

1. Introduction

Existing structures located on soft and liquefiable sites are often founded on piles. The performance of piles after major earthquakes, especially where liquefiable soils are present, has been widely reported [1]. Case histories have shown that piles develop plastic hinges at locations between liquefied and non-liquefied soil layers (due to the high stiffness differential), which causes large kinematic loading on piles. Assessing earthquake pile performance is difficult considering that the piles cannot be inspected immediately after an earthquake, especially if the structure shows no apparent indication of foundation failure (e.g. tilting). There have been cases where the structures remained in service after a major earthquake and, at a later stage, the piles were found to be extensively damaged (e.g. 1964 Niigata earthquake, see Fig. 1 from [2]).

This paper presents the assessment of the pile foundation of an LPG spherical tank located in a site with liquefiable soil layers, where it was found that the piles would shear off under earthquake excitation corresponding to a PGA of 0.45g. According to performance based approaches (refer to ASCE Guidelines), LPG storage tanks are considered to be essential[1] as they contain extremely hazardous materials. Design guidelines generally recommend that essential structures should maintain their structural integrity and be able to maintain containment of hazardous materials after a design earthquake [3]. Therefore, if these structures were founded on piles and there is the presence of liquefiable soils in the site, a pile performance as shown in Fig. 1 would be unacceptable. As pile failure is considered unacceptable, a retrofit study was performed to assess the effectiveness of an in-ground ringwall concept using overlapping jet grout columns, surrounding the pile foundation, in minimizing the kinematic pile loading. DSSI analyses using finite elements were performed for both the initial vulnerability assessment of the pile foundation and the retrofit study.

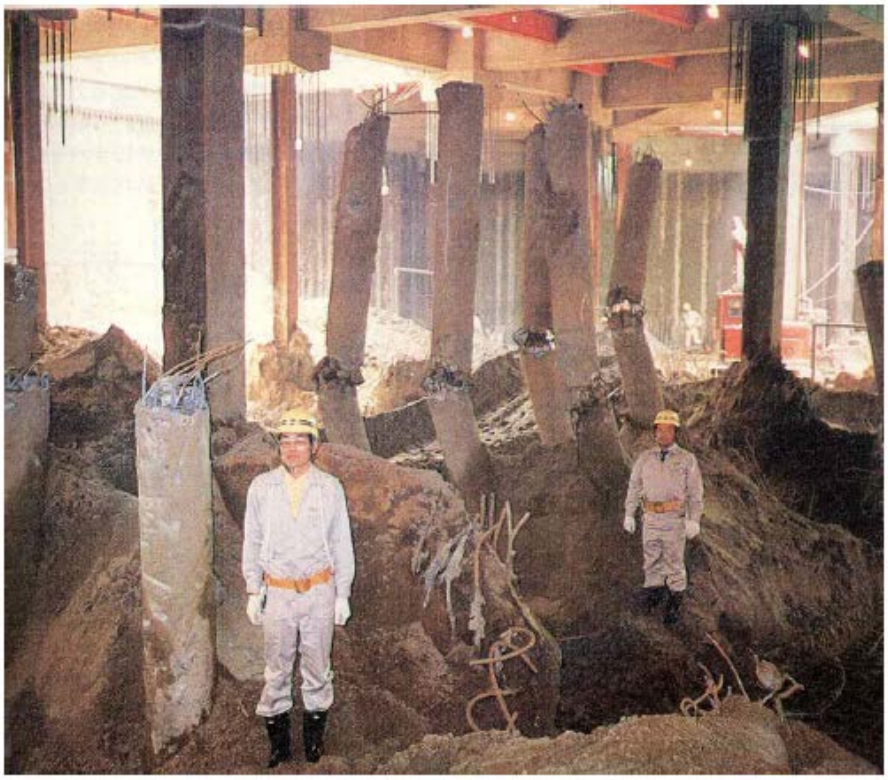

Fig. 1 – Earthquake damage on piles, from [2].

[1] Essential facilities, as defined by ASCE Guidelines [3], are those structures containing extremely hazardous materials that pose a threat to the public if released.

2. Structure and Foundations

The above-ground structure considered in this study consists of a 17.9m diameter LPG spherical tank mounted on a reinforced concrete raft (see view of finite element model in Fig. 2). The sphere itself is supported on 10 steel circular hollow section columns (CHS 864mm diameter/9.5mm thickness) with a yield strength of 250MPa (ASTM A36 Steel). The columns are cross braced with 305x38mm steel plate members with a yield strength of 260MPa (ASTM A516-70 Steel).

The tank content has a total mass of 1,685t when full, based on a product density of 560kg/m^3. The mass of the tank's appendages (e.g. stairway, handrail, inspection scaffold, etc.) was considered to be relatively small in comparison to the mass of the tank and its contents (see typical LPG spherical tank in Fig. 2, from [4]). Therefore, this mass was neglected in the modelling of the tank.

The LPG spherical tank foundation consists of a reinforced concrete octagonal ring (22.4m outer and 4.55m inner plan dimensions), supported on 60 precast pre-stressed concrete piles. The piles have a 355mm x 355mm square cross section and are 25m in length. The prestress reinforcement consists of eight 12.5mm diameter prestressed steel strands (ASTM A416 seven-wire strands), with a minimum breaking strength of 1,860MPa.

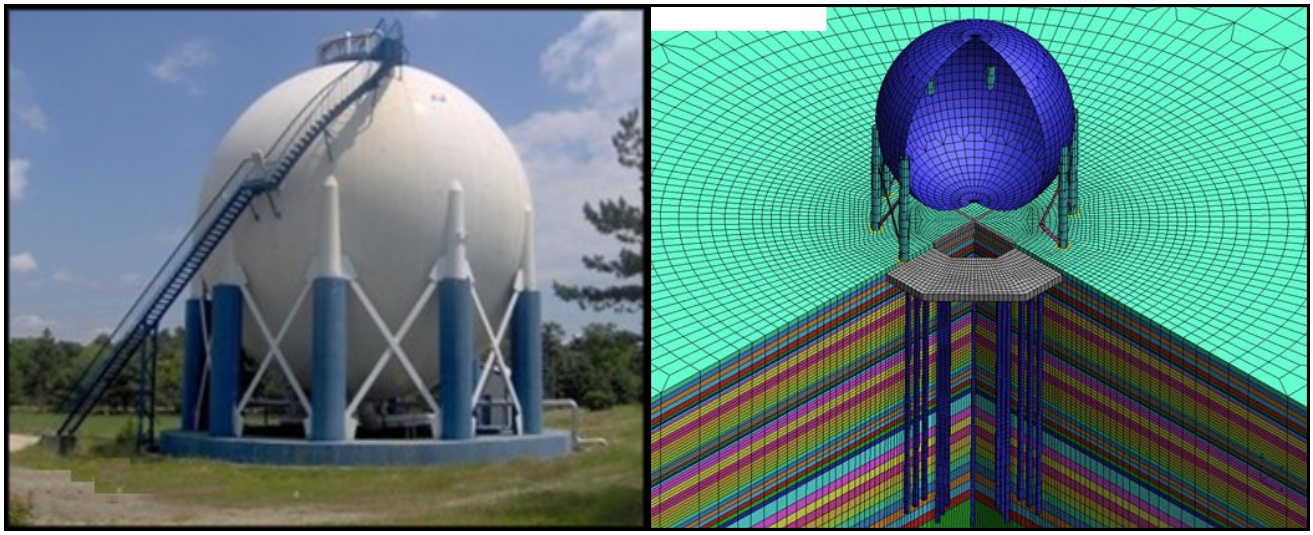

Fig. 2 – Typical LPG spherical tank, from [4] (left); and close-up view of the 3D finite element model in LS-DYNA of the studied spherical tank (right).

3. Site Conditions

A simplified ground model was derived for this study based on borehole data available from two borings. The data available included: (i) geological borehole log descriptions; (ii) Atterberg limits results in terms of Plasticity Index (PI); (iii) particle size distribution (PSD) results in terms of Fines Content (FC%); and (iv) SPT-N measurements. Fig. 3 illustrates a summary of the simplified soil stratigraphy.

The sand layers were considered to be likely to liquefy if the SPT-N values were found to be below the threshold values corresponding to liquefaction factors of safety (FS = Capacity/Demand) of 1.0 and 1.25, per the recommended procedure in [5] for ground motions corresponding to a design 7.5M_w event. Sensitivity analyses using best estimate, upper, and lower bound profiles, as well as the assumed governing earthquake magnitude (M_w = 7.5), were performed in order to approximate the likely thickness of the liquefiable layers. The sensitivity studies indicated that sand layers at depths: 3-4m (Upper Liquefied Layer), 8-10m (Middle Liquefied Layer), and 15-18.5m (Lower Liquefied Layer) below ground surface (b.g.s.) would liquefy (see Fig. 3). It is anticipated that the liquefiable layers would lose stiffness and strength during ground excitation. To incorporate the loss of stiffness and strength of these soil layers in the analysis, residual shear strengths ($S_{u,r}$) were estimated based on

the SPT-N values according to the empirical correlation in [6]. The $S_{u,r}$ value for the two uppermost liquefied layers was estimated as 5kPa; whereas for the lowermost liquefied layer, it was estimated as 25kPa. Parameters such as the small-strain shear modulus (G_0) and the modulus degradation (G/G_0) curves were selected to ensure that the maximum shear stress mobilized in the liquefied soil does not exceed $S_{u,r}$.

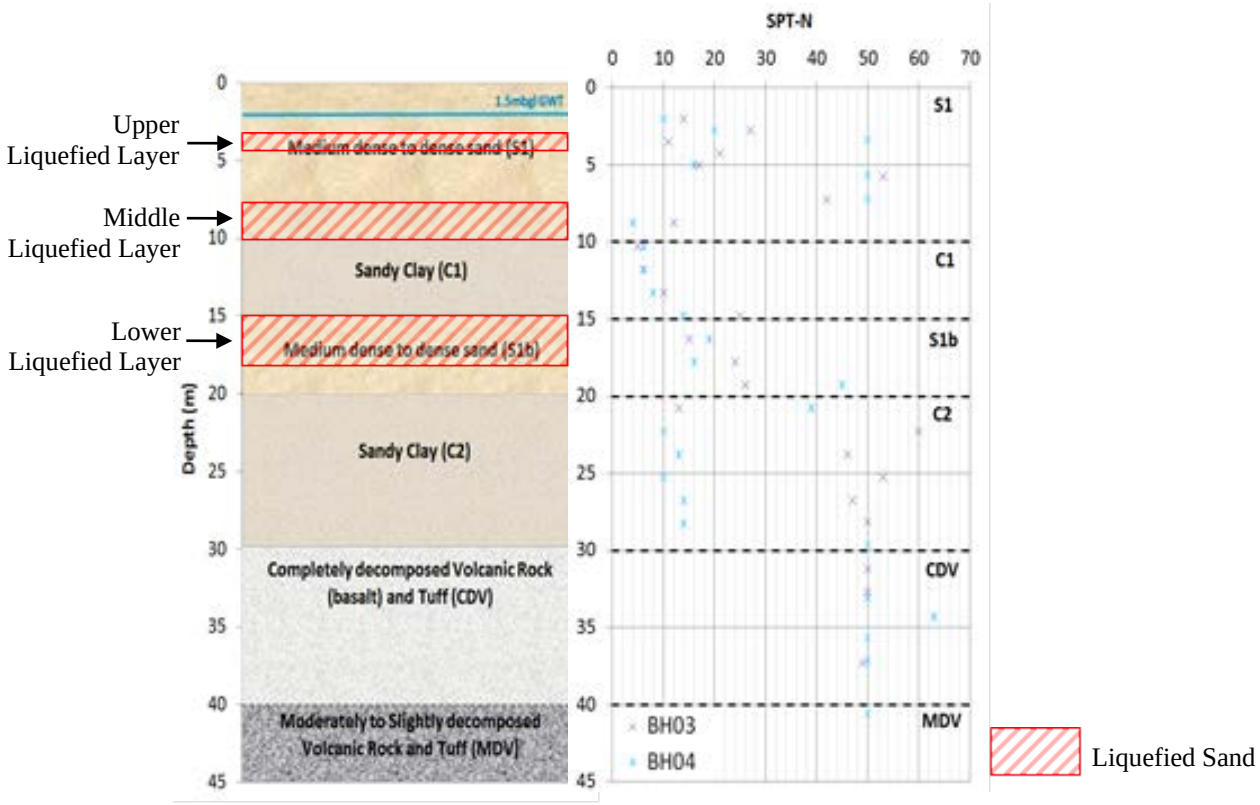

Fig. 3 – Summary of the simplified soil stratigraphy.

4. Finite Element Model for Dynamic Soil-Structure Interaction Analysis

A three-dimensional finite element model was developed for dynamic soil-structure interaction (DSSI) analysis using the direct method [7]. The equations of motion are directly solved in the time domain, this allows the simultaneous treatment of non-linearity of the structure, piles, soil, and pile-soil interaction. The loading on the piles from the inertial effects of the superstructure and from the kinematic soil movement are coupled in the analysis.

The DSSI model consists of the above-ground structural model or superstructure, the below-ground foundation or substructure, and the soil model. Fig. 4 shows the 3D finite element model of the LPG spherical tank. The general purpose 3D non-linear finite element program LS-DYNA [8] was used to perform the DSSI analysis. LS-DYNA has been previously used for a wide range of foundation and soil-structure interaction problems [9].

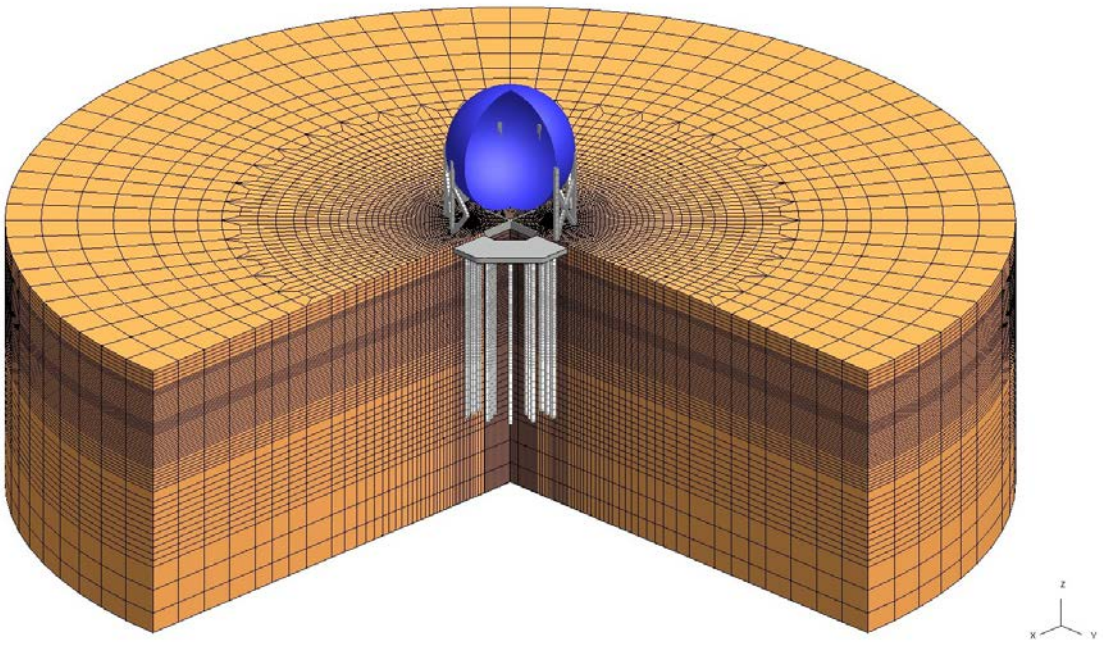

Fig. 4 – Cut-out view of 3D finite element model of the LPG spherical tank in LS-DYNA.

4.1 Superstructure Modelling

The tank sphere was modelled rigidly considering a constant shell thickness of 46.5mm. The thickness used was in accordance with average values of typical LPG spherical tanks of this size. The contents of the tank was modelled using a lumped mass located at the center of the sphere, rigidly constrained to the tank wall. The mass of the tank's appendages was neglected.

The CHS columns and cross braces were modelled with elastic-perfectly plastic beam elements. The CHS columns were rotationally fixed to the sphere and the concrete plinths; whereas the cross braces were pinned both at their connection to the columns and to each other where they cross over.

4.2 Foundation Modelling

The concrete raft was modelled with linear-elastic solid element with Young's modulus, E, of 22.6GPa and Poisson's ratio, ν, of 0.2.

The piles were modelled with non-linear beam elements that capture cyclic behavior, and they were pinned at their connection to the concrete raft. Their cross section capacity, both in the form of interaction diagram and moment-rotation capacity curve, were estimated using the computer program XTRACT [10]. The piles were modelled with their expected yield strength rather than with their design yield strength (i.e. no strength reduction factors were applied).

The piles respond elastically as long as the combination of the bending moment (M) and axial force (N) on the piles lies within the M-N interaction diagram (see Fig. 5a). Once the M-N pair reaches the yield envelope, a plastic hinge forms and inelastic rotation will take place until concrete crushing occurs and the pile's moment resistance decreases in a brittle manner. This plastic rotation limit is the rotation that can safely respond to the seismic demand, and was estimated to be 9.83×10^{-3}rad (see Fig. 5b).

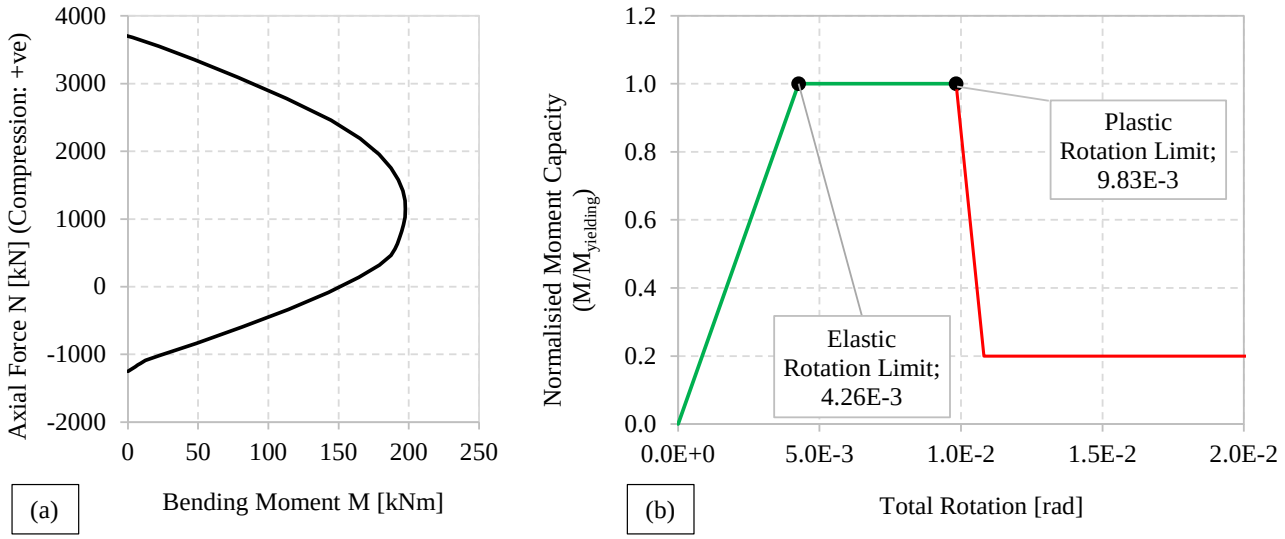

Fig. 5 – M-N Interaction Diagram (a), and Moment-Rotation capacity curve (b) for the 355mm SQ precast piles.

4.3 Soil Modelling

The soil model consists of 8-noded solid elements using LS-DYNA's non-linear soil material model MAT_HYSTERETIC_SOIL [8]. This model captures the hysteresis of the soil under cyclic loading by means of an input nested surface consisting of 10 superimposed 'layers' of elastoplastic materials, each with its own value of elastic modulus and yield stress, thus defining the backbone curve (shear strain vs shear stress). It has been previously used in soil-structure interaction and site response studies (e.g. [11] and [12]). Both the liquefied and non-liquefied soil layers have been modeled using this material model. The modeling parameters for the liquefied layers were based on residual strengths $S_{u,r}$ as described in Section 3. Note that using liquefied soil properties from the beginning of the analysis is conservative. A shear strength reduction occurs over the duration of the seismic excitation.

The soil-pile interaction has been modeled by means of 'virtual' springs capturing the pile skin friction (t-z), end bearing (Q-z), and lateral (p-y) response. The lateral pile response for the non-liquefied layers was modeled using their soil parameters ϕ' and S_u of sands and clays, respectively. For the liquefied sand layers, their estimated residual strengths $S_{u,r}$ were used, assuming p-y relationships for clays as suggested in [13].

4.4 Boundary Conditions

The soil block model had a non-reflecting boundary condition at bedrock level using the method in [14]. This lower artificial boundary represents an infinite half space that was not modelled explicitly. Discrete viscous damper elements in each horizontal direction were included at the bedrock level, with properties from the bedrock characteristic of the area.

The cylindrical soil block model had dimensions of 140m diameter and 40m depth. The dimensions of the soil block were chosen to be sufficiently large to ensure free-field conditions at the edge of the model.

Each soil layer perimeter node set was constrained so as not to allow relative displacement. Each constraint was also globally restrained from rotation. The base of the model was fixed in the vertical direction, but was subjected to bi-axial earthquake excitation along the two orthogonal horizontal directions (X and Y axes). The time history pair used in the analysis was matched to a 475-year return period rock design spectrum with a peak ground acceleration (PGA) of 0.45g, which was input to the base of the model.

5. DSSI Analysis Results

Considering the site conditions presented in Section 3, it was anticipated that lateral soil deformations would concentrate on either one of the liquefied sand layers shown in Fig. 3. Results of the DSSI analysis showed that

it was the middle liquefied layer (at a depth of around 10m below ground surface) that concentrated most of the lateral soil deformations (~200mm; see Fig. 6). The middle liquefied layer created a non-liquefied 'crust' that imposed additional lateral deformation on the upper part of the piles.

The DSSI analysis showed that the piles exceeded their capacity where most of the lateral soil deformations were concentrated (i.e. the mid-liquefied layer), and plastic hinges formed. Furthermore, following inelastic rotations of the plastic hinges during shaking, the plastic rotation capacity of 9.83×10^{-3}rad of the piles was far exceeded, suggesting that the piles would shear off at these locations (see Fig. 6).

Whilst there have been cases where structures have remained in service in spite of damaged pile foundations, the risk of foundation failure in petrochemical facilities is considered to be unacceptable. Therefore, a mitigation solution was studied to reduce the kinematic loading on piles due to liquefied soil layers.

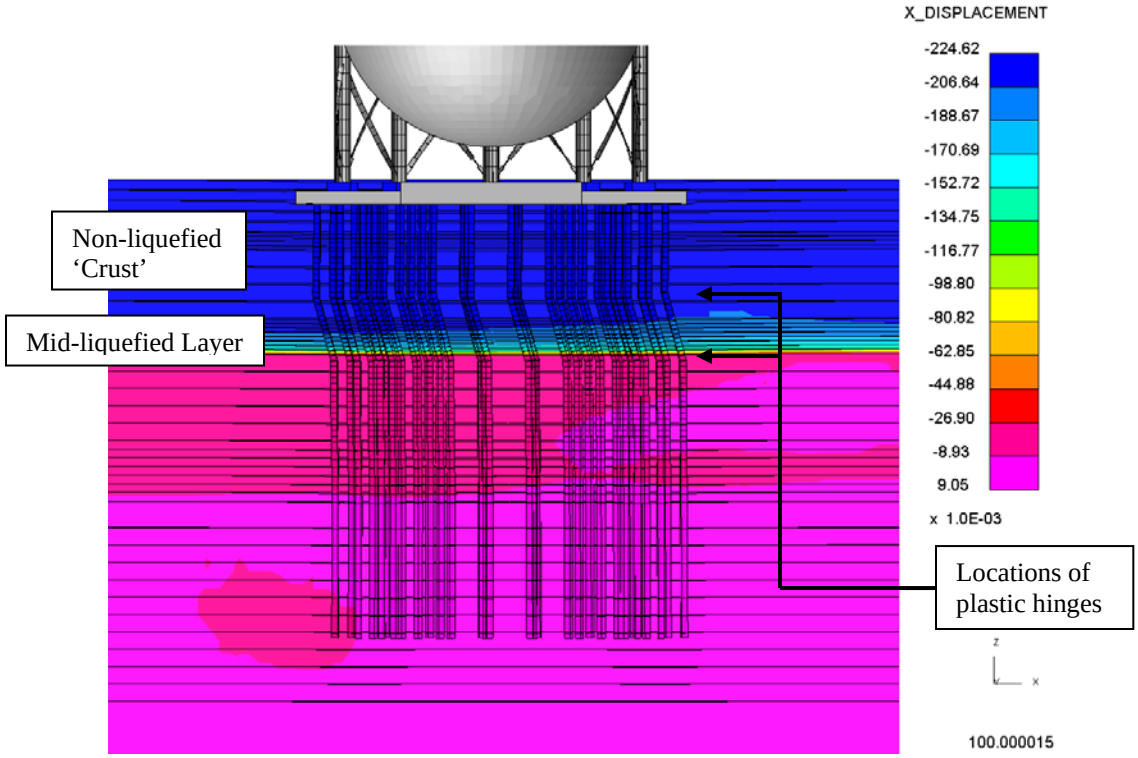

Fig. 6 – Soil lateral displacements showing kinematic effect on piles due to liquefied soil layer. Displacement units: m. NB: Exaggerated deformations.

6. Proposed Mitigation Measure and Optimization

The proposed mitigation solution for reducing the kinematic loading on the piles consisted of an in-ground ringwall surrounding the pile foundation (see Fig. 7a). Other studies available in the literature have presented liquefaction mitigation solutions based on rigid (e.g. concrete) containment walls and secant pile walls (e.g. [15] and [16]). The in-ground ringwall concept presented herein however, would be composed of overlapping jet grout columns that, depending on the thickness of the wall required, could be made of two rows or a single row of overlapping columns (see Fig. 7b). Single jet grout columns are generally brittle; however, when combined to form a circular wall, the jet grout wall provides a relatively rigid inclusion that deflects soil deformation. Therefore, this in-ground ringwall system will shield the piles from the kinematic loading. The jet grout column system was selected based on:

a) The governing action on piles (i.e. kinematic loading);

b) Constructability (i.e. ease of access, size of construction equipment, etc.);

c) Capability of local contractors; and

d) Relative ease of construction verification.

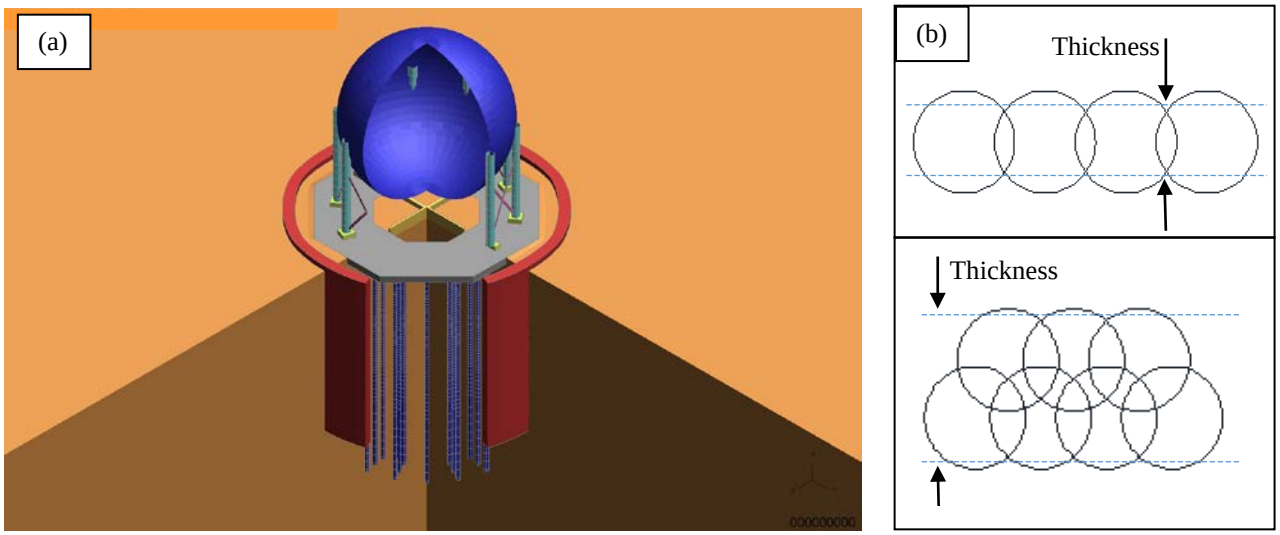

Fig. 7 – (a) Close-up view of the 3D finite element model in LS-DYNA of the studied spherical tank including the in-ground jet grout ringwall (NB: The top soil layer is not shown here for visualization purposes only). (b) Plan layout of single- and double-row overlapping columns.

Prior to incorporating the in-ground ringwall into the DSSI finite element model for verifying the effectiveness of the system, a scoping study was performed to optimize the dimensions of the in-ground wall (i.e. thickness and length required to minimize damage on the wall). A finite element model consisting only of the in-ground ringwall embedded in the existing soil block model (i.e. no superstructure or foundation) was subjected to a lateral pushover-like analysis by means of prescribed displacements applied to the edge of the soil block (see Fig. 8a). The applied displacements were consistent with the expected soil deformations shown in Fig. 6.

The in-ground ringwall finite element model consisted of 8-noded solid elements using the Mohr-Coulomb soil model. The parameters used to define the Mohr-Coulomb model are shown in Table 1 and were conservatively chosen from published literature (e.g. [17] and [18]).

Table 1 – Mohr-Coulomb soil model parameters for in-ground ringwall model

Cohesion value (shear strength at zero normal stress) [C]	**Angle of friction [ϕ]**	**Elastic shear modulus [G]**	**Poisson's ratio [ν]**	**Mass density [ρ]**
1.40MPa	0.001rad	333MPa	0.2	2,000kg/m^3

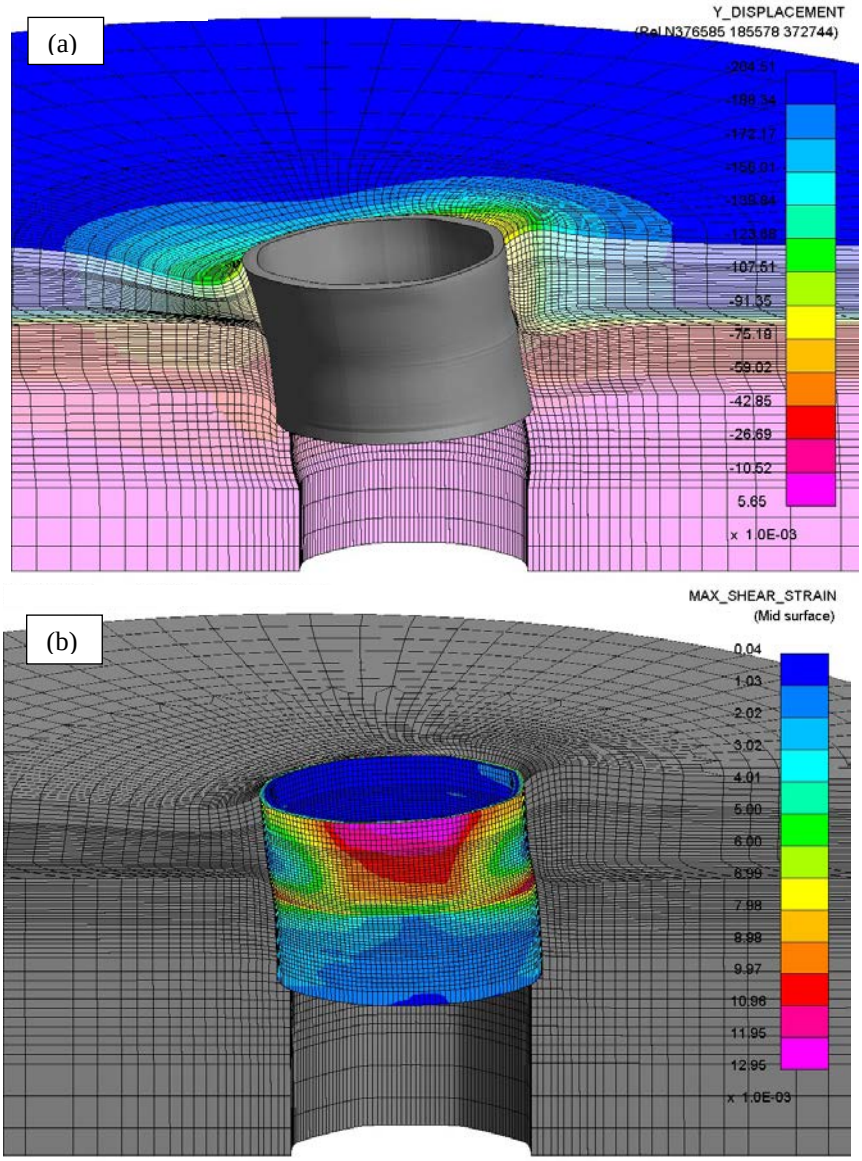

Fig. 8 – Applied lateral soil displacement loading on in-ground wall (a) – units: m; and maximum shear strains on 20m long, 1.2m thick in-ground ringwall under pushover-like lateral analysis (b).
NB: Exaggerated deformations.

The scoping study aimed to find suitable dimensions for the ringwall by limiting the maximum shear stresses on the wall to be less than 1.40MPa, and the maximum shear strains to be less than 1%. The zone of interest was at the depth where the high soil deformations were encountered in the DSSI analysis due to a liquefied layer (at around 10m below ground surface, see Fig. 6). The scoping study showed that in-ground ringwalls significantly reduced the lateral soil deformations in the vicinity of the structure, compared to the applied lateral soil displacements at the edge of the soil block model (see Fig. 8a). Lateral deformations were reduced from about 200mm down to 90mm. The soil immediately outside the in-ground ringwall generally flows around the ringwall to accommodate the decrease in lateral deformations. The scoping study found that two configurations: (i) 15m long, 1.2m thick, and (ii) 20m long, 1.2m thick ringwalls would have shear stresses and strains within the established limits (e.g. see Fig. 8b). Considering that the model for the scoping study consisted of only the in-ground ringwall and the soil block (i.e. no concrete raft acting as a diaphragm at the top of the wall), the relatively high shear strains (>1%) at the top of the wall were ignored. Therefore, the two in-ground

ringwall layouts were incorporated into the existing finite element model to test the effectiveness of the mitigation measure.

7. Verification of Mitigation Measure

Finite element models including the jet grout in-ground ringwall (see Fig. 7a) for the two options presented in the previous section were subjected to the same pair of orthogonal time histories in LS-DYNA.

The results of the DSSI analysis of the 15m long, 1.2m thick ringwall option showed that, although the ringwall stresses and strains remained under the established limits, the failure mechanism of the piles changed altogether. The piles that originally failed at a depth of around 10m below ground surface. (i.e. the mid-liquefied layer), when no ringwall was considered, now fail at a depth of around 18.5m below ground surface. (i.e. the lower-liquefied layer). It is clear that the 15m long ringwall does not have sufficient length to completely shield the piles against kinematic loading due to the lower-liquefied layer.

On the other hand, the results of the DSSI analysis of the 20m long, 1.2m thick ringwall option showed that the piles remained elastic, whilst the ringwall stresses and strains remained under the established limits. This longer in-ground ringwall option greatly reduced the kinematic loading on the piles. Fig. 9 compares the performance of the piles with no ringwall to that with the 20m long, 1.2m thick in-ground ringwall solution.

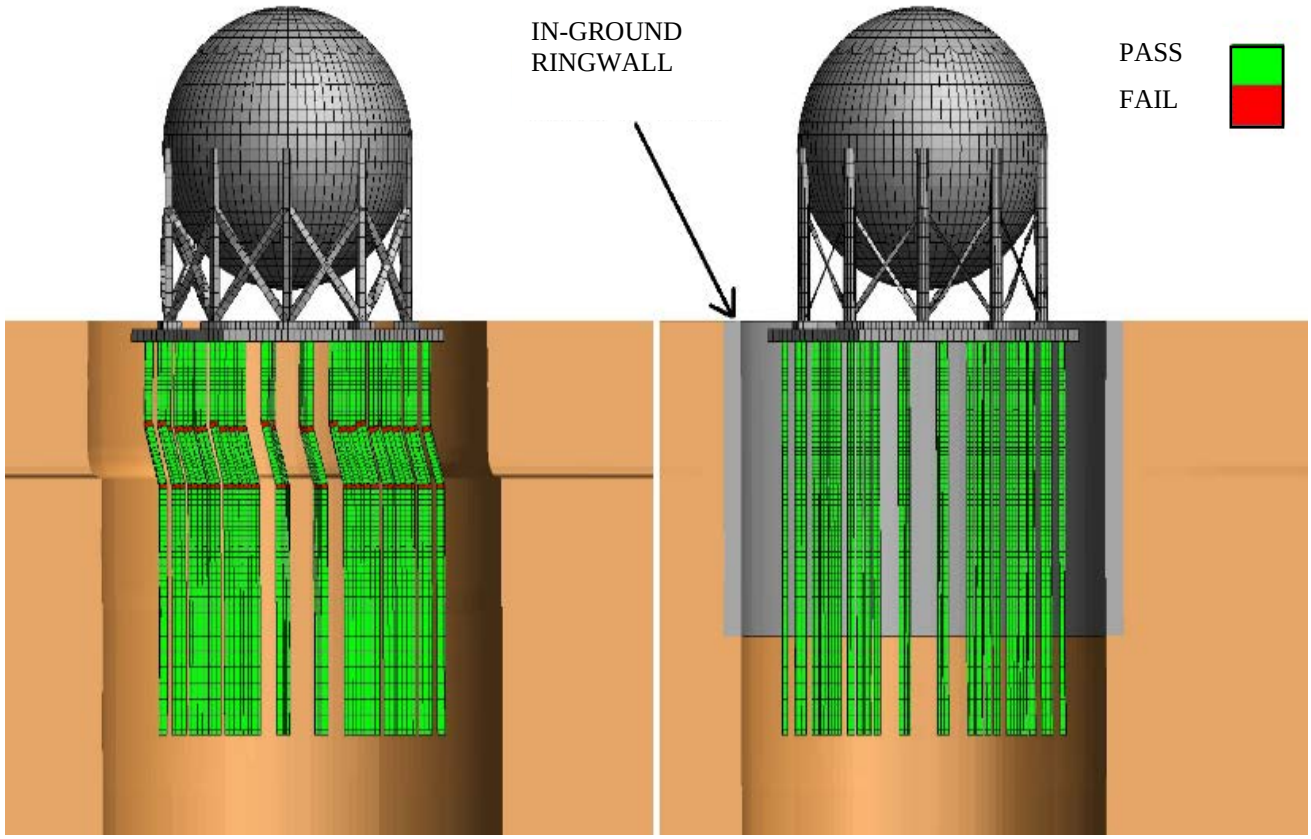

Fig. 9 – Comparison of pile performance, in terms of rotation magnitudes, between DSSI analysis without in-ground wall (left) and with in-ground wall (right). Red indicates exceedance of plastic rotation capacity. NB: Exaggerated deformations.

8. Conclusions

The finite element DSSI analyses provided 'proof of concept' showing that in-ground ringwalls, sufficiently embedded into non-liquefiable soils, can significantly reduce kinematic loading and can be used to retrofit existing foundations in sites with potentially liquefiable soils.

Special attention must be given to possible changes in failure mechanism when proposing mitigation measures. A mitigation solution may solve a problem at a certain location, but other elements that were originally within their capacities may then fail.

Whilst it was found that a 20m long, 1.2m thick in-ground ringwall concept is a technically viable solution in this particular study, additional geotechnical data may help to optimize the ringwall dimensions given the number of assumptions made, especially for the liquefaction potential evaluation of the sand layers and the reduced soil properties assigned to them.

9. Acknowledgements

The authors thank the contributions of Sundip Shah and Michael Vasileiadis from Arup, who formed part of the team that performed the analyses presented in this paper; and also thank Richard Sturt and Anton Pillai from Arup for their technical support throughout the analyses.

10. References

[1] Meymand, PJ (1998): Shaking Table Scale Model Tests of Nonlinear Soil-Pile-Superstructure Interaction in Soft Clay. *PhD Thesis*, University of California, Berkeley.

[2] Hamada M (1991): Damage to Piles by Liquefaction-Induced Ground Displacements. *3rd U.S. Conference Lifeline Earthquake Engineering*, ASCE, Los Angeles, USA, 1172-1181.

[3] ASCE (2011): Guidelines for Seismic Evaluation and Design of Petrochemical Facilities, 2nd Edition. American Society of Civil Engineers, Virginia, USA.

[4] China Tanks and Vessels (2016): LPG Spherical Tanks. [ONLINE] Available at: http://www.chinatanksandvessel.com/lpg-spherical-tanks.html. [Accessed 15 April 2016].

[5] Youd YT (2001): Liquefaction Resistance of Soils: Summary Report from the 1996 NCEER and 1998 NCEER/NSF Workshops on Evaluation of Liquefaction Resistance of Soils. *Journal of Geotechnical and Geoenvironmental Engineering*, 127(10), 817-833.

[6] Seed RB, Harder LF (1990): SPT-based analysis of cyclic pore pressure generation and undrained residual strength. *H. Bolton Memorial Symposium. 2*, pp. 351-376. University of California, Berkeley.

[7] Kramer S (1996): *Geotechnical Earthquake Engineering*. Prentice-Hall, 1st edition.

[8] Livermore Software Technology Corporation – LSTC (2012): LS-DYNA Keyword user's manual, Version 971, R6.0.0, Volume I & II.

[9] Lubkowski ZA, Pappin JW, Willford MR (2000): The influence of dynamic soil structure interaction on the seismic design and performance of an ethylene tank. *12th World Conference in Earthquake Engineering*, Auckland, New Zealand.

[10] Chadwell CB (2002): XTRACT, Cross Section Analysis Software for Structural and Earthquake Engineering. Imbsen & Associates.

[11] Ellison KC, Masroor AM, Almufti I, Willford M, O'Riordan N (2015): Structure-Soil-Structure Interaction Analysis in a Highly Seismic, Dense Urban Regeneration Zone. *6th International Conference on Earthquake Geotechnical Engineering*, Christchurch, New Zealand.

[12] Bolisetti C, Whittaker AS, Mason HB, Almufti I, Willford M (2014): Equivalent linear and nonlinear site response analysis for design and risk assessment of safety-related nuclear structures. *Nuclear Engineering and Design*, 275, 107-121.

[13] Ashford SA, Boulanger RW, Brandenberg SJ (2011): Recommended Design Practice for Pile Foundations in Laterally Spreading Ground. *Pacific Earthquake Engineering Research Center, PEER Report 2011/04*, Berkeley, USA.

[14] Lysmer J (1978): Analytical procedures in soil dynamics. *Earthquake Engineering Research Center, Report No. UCB/EERC-78/29*, Berkeley, USA.

[15] Mitrani H, Madabhushi SPG (2012): Rigid Containment Walls for Liquefaction Remediation. *Journal of Earthquake and Tsunami*, 6(4).

[16] Saez E, Ledezma C (2015): Liquefaction mitigation using secant piles wall under a large water tank. Soil Dynamics and Earthquake Engineering, 79(B), 415-428.

[17] Modoni G, Bzowka J (2012): Analysis of Foundations Reinforced with Jet Grouting. *Journal of Geotechnical and Geoenvironmental Engineering © ASCE*, 138, 1442-1454.

[18] Axtell PJ, Stark TD (2008): Increase in Shear Modulus by Soil Mix and Jet Grout Methods. *DFI Journal – The Journal of the Deep Foundations Institute*, 2(1), 11-21.